

Correlations drive the attosecond response of strongly-correlated insulators

Romain Cazali,^{1,*} Amina Alic,^{2,*} Matthieu Guer,¹ Christopher J. Kaplan,³
 Fabien Lepetit,¹ Olivier Tcherbakoff,¹ Stéphane Guizard,^{1,4} Angel Rubio,^{5,6,7}
 Nicolas Tancogne-Dejean,^{5,6} Gheorghe S. Chiuzbăian,² and Romain Géneaux^{1,4,†}

¹*Université Paris-Saclay, CEA, LIDYL, 91191 Gif-sur-Yvette, France*

²*Sorbonne Université, CNRS, Laboratoire de Chimie Physique
 - Matière et Rayonnement, LCPMR, 75005 Paris, France*

³*Department of Chemistry, University of California, Berkeley, 94720, USA*

⁴*CY Cergy Paris Université, CEA, LIDYL, 91191 Gif-sur-Yvette, France*

⁵*Max Planck Institute for the Structure and Dynamics of Matter,
 Luruper Chaussee 149, 22761 Hamburg, Germany*

⁶*Center for Free-Electron Laser Science CFEL,
 Deutsches Elektronen-Synchrotron DESY, Notkestraße 85, 22607 Hamburg, Germany*

⁷*Center for Computational Quantum Physics (CCQ),
 The Flatiron Institute, 162 Fifth Avenue, New York NY 10010, USA*

Attosecond spectroscopy of materials has provided invaluable insight into light-driven coherent electron dynamics. However, attosecond spectroscopies have so far been focused on weakly-correlated materials. As a result, the behavior of strongly-correlated systems is largely unknown at sub- to few-femtosecond timescales, even though it is typically the realm at which electron-electron interactions operate. Here we conduct attosecond-resolved experiments on the correlated insulator nickel oxide, and compare its response to a common band insulator, revealing fundamentally different behaviors. The results, together with state-of-the-art time-dependent *ab initio* calculations, show that the correlated system response is governed by a laser-driven quench of electron correlations. The evolution of the on-site electronic interaction is measured here at its natural timescale, marking the first direct measurement of Hubbard U renormalization in NiO. It is found to take place within a few femtoseconds, after which structural changes slowly start to take place. The resulting picture sheds light on the entire light-induced response of a strongly-correlated system, from attosecond to long-lived effects.

* These two authors contributed equally

† romain.geneaux@cea.fr

Strongly correlated materials present peculiar behavior of both technological and fundamental interest,^{1,2} which stems from the strong repulsive electron-electron interaction, as well as strong coupling between charge, spin, orbital, and lattice degrees of freedom. Because of these highly intertwined order parameters, excitation with laser pulses offers striking control possibilities, such as light-induced phase transitions³⁻⁵ and superconductivity,^{6,7} access to non-thermal states^{8,9} and the creation of Floquet-Bloch states.¹⁰ The Hubbard U parameter quantifies the effective on-site Coulomb repulsion between electrons, a key factor governing correlated electronic systems. In transition metal oxides, U has values of several electron-volts, meaning that correlated electron dynamics are expected to take place on timescales of $\hbar/U \simeq 0.1-1$ fs.¹¹ Therefore, strong correlations might facilitate the control of parameters and phases of materials at exceptionally high speeds, using light fields with optical cycles of a few femtoseconds.

Understanding non-equilibrium dynamics in correlated materials at ultrashort timescales is crucial for advancing technologies reliant on ultrafast electronic switching and phase control. Despite their transformative potential, the response of these systems under strong light fields remains poorly understood. Theoretically, standard first-principle calculations suffer from difficulties when adapting existing adiabatic pictures to highly out-of-equilibrium dynamics. Experimentally, accessing these timescales requires attosecond resolution. While state-of-the-art attosecond experiments can now explain the sub-cycle response of weakly-correlated semiconductors^{12,13} and band insulators,^{14,15} most existing descriptions rely on single-particle pictures or simplified few-band models. For instance, the dynamical Franz-Keldysh effect,¹⁵⁻¹⁷ a key transient effect at the attosecond scale, is explained as a field-induced modification of the single-particle band structure. This description is expected to break down when many-body processes dominate the optical response of the materials. Therefore, the response of strongly correlated solids to intense light fields on few- and sub-femtosecond timescales remains unknown. Do electronic correlations amplify the sub-optical-cycle dynamics under an external light pulse, or do they suppress the ultrafast response by enhancing electromagnetic field screening?

In order to answer this question, we perform attosecond-resolved measurements on a band insulator and a correlated insulator, in exactly the same conditions. We choose two simple test-bed materials: magnesium oxide, a prototypical weakly-correlated metal oxide, and nickel oxide, which is historically the first system identified as a strongly-correlated insulator.¹⁸ Unlike some other correlated materials,³ nickel oxide does not undergo any light-induced phase transition and thus offers the advantage of decoupled electronic and structural orders at short times. Our results reveal completely different light-induced responses between the two oxides at the attosecond timescale: while MgO shows only transient reversible effects, NiO exhibits purely long-lived changes without visible subcycle dynamics. This shows that existing intuitive single-particle based pictures of insulators cannot be applied to nickel oxide, and fail to predict its response to intense light excitations. Instead, the response of NiO is explained by a light-driven quench of the on-site correlations, meaning that the intense laser field dynamically reduces the electron-electron

interactions, as revealed by our *ab initio* simulations based on real-time TDDFT complemented by an effective Hubbard U .^{19,20} Following this interpretation, the measurement gives a direct access to the light-driven renormalization of the Hubbard U on its true timescale, evidencing an ultrafast electronic response of only a few femtoseconds. Additionally, we follow the NiO response up to 50 ps and observe the relaxation corresponding to the formation of a structurally distorted non-thermal lattice state. These measurements represent the first experimental observation of the birth of a non-thermal state driven by correlations, with the observation of the sub-femtosecond correlated electronic response, up to the long-lived picosecond dynamics of the metastable state induced by light.

Comparing correlated and band insulators

To explore the light-driven response of NiO and MgO, we perform pump-probe experiments according to the attosecond transient reflectivity scheme.²¹ Attosecond pulses with spectra spanning 40–72 eV impinge on the monocrystalline sample with an angle of 65° from normal (see Fig 1a and Methods for details on the experimental setup). Fig. 1d,e display the static reflectivity of the samples, showing either the Mg $L_{2,3}$ or the Ni $M_{2,3}$ edges. The sample is then excited by a p-polarized 5 fs laser pulse with an incident intensity of 6 TW cm^{-2} and a central photon energy of 1.58 eV. The pump-probe delay is actively stabilized, guaranteeing a stability of 100 as over the course of the measurement. Fig. 1b,c displays the band structure of both systems around the Γ point, illustrating that the bandgaps (7.8 eV for MgO²² and 4.3 eV for NiO²³) are larger than the pump energy. It shows a key difference between the two insulators: the first NiO conduction band (which corresponds to the $3d e_g$ orbitals) is much flatter than the one of MgO, corresponding to more localized electron density in real space and thus stronger correlations.

Starting with the more conventional case of the band insulator MgO, Figure 2a shows its attosecond transient reflectivity. The strong driving field induces large reflectivity change ($\approx 20\%$) localized around the temporal overlap, as previously reported in Ref.²⁴ In addition, oscillations with 1.3 fs period are resolved across the entire spectrum (Fig. 2c), corresponding to half the driving electric field period. This is typical of the Dynamical Franz-Keldysh Effect (DFKE), which has been identified in the band insulators diamond¹⁵ and SiO₂,¹⁷ here with additional excitonic signatures as observed and analyzed in details in MgF₂.²⁵ The DFKE is a field-driven change of the absorption of a material near its bandgap, giving rise to shifts and satellite features that both oscillate in synchrony with the laser electric field. It is noteworthy that this effect is accurately described by perturbation theory applied to the static electroabsorption coefficient,¹⁶ which is well-suited to weakly-correlated materials such as MgO. While a detailed study of these oscillations is not the topic of this paper, the measurement effectively exemplifies the behavior of a bandgap insulator, and provides an important reference measurement of the instrument temporal resolution.

Keeping identical experimental conditions – pump fluence, duration, and probing scheme – Figure 2b displays the same quantity for NiO. Figure 2d shows a temporal lineout of the main observed feature. The response of NiO has several significant differences compared to MgO: (i) the pump-induced reflectivity change is much weaker ($\approx 4\%$), (ii) the material response rises more slowly, and persists after excitation

and (iii) no field-driven oscillations are resolved when the pump pulse is active. These observations already clearly suggests that the two systems behave fundamentally differently upon photo-excitation. We note that at reduced pump intensity, the NiO response decreased in magnitude, but kept the same characteristics and spectral shape. In order to explain this response, we perform a detailed analysis of the spectral changes of the Ni $M_{2,3}$ edge. Because the measurement is performed in reflection geometry, we apply a Kramers-Kronig treatment of the data in order to extract the absorption coefficient. The absolute reflectivity of the sample (Fig. 1c) is padded with literature data to cover the visible to x-ray range,²⁴ before applying a variational Kramers-Kronig algorithm.²⁶ The obtained absorption coefficient matches well with synchrotron measurements.²⁷ Figure 2e compares the obtained transient absorption at positive delays with a pure redshift of -51 meV, displaying a remarkable match. At all time delays, the transient absorption trace is extremely well reproduced by a pure rigid shift of the absorption edge. The absence of more complex features, such as broadening or the appearance of new band-like signals, suggest that the signal does not stem from carrier photoinjection²⁸ or heating.²⁹ Because the spectral change is so simple, even the transient reflectivity signal is well described by a pure redshift of the same amount, as shown in Figure 2f. This allows us to conclude that the pump-induced response at the M-edge can be described purely as a redshift.

Ultrafast renormalization of Hubbard U

This observation evokes the possibility that the main effect at play is a light-induced shift of the NiO conduction band (CB). In strongly correlated systems, this has been shown to be a consequence of a laser-induced reduction of the Hubbard U , thereby shifting the upper Hubbard band (UHB, which is the CB in NiO) down in energy. This so-called U renormalization was predicted theoretically for NiO^{19,20} but to date, experiments on NiO were performed using free-electron lasers,³⁰⁻³² which lack the sufficient temporal resolution to confirm the prediction. On the other hand, the clear transient renormalization of U was observed experimentally in a transition metal dichalcogenide³³ and in a cuprate superconductor,³⁴ but so far without the possibility to directly follow its temporal evolution. In order to explore this possible scenario, we perform advanced theoretical simulations. Modeling the experiment accurately is quite challenging: it requires describing out-of-equilibrium electronic motion in the presence of strong correlations and non-linear optical excitation. In addition, it requires computing the time-dependent XUV reflectivity with sufficient time-resolution. We resort to time-dependent density functional theory plus Hubbard U (TDDFT + U), including all necessary core levels, coupled to macroscopic Maxwell equations. This approach provides a good balance between computational efficiency and accuracy in describing real systems.³⁵ We use the same pump pulse duration and fluence as in the experiment, making the calculation entirely *ab initio*. Figures 3a,b compare the transient reflectivity signal measured experimentally and obtained theoretically with the same color scale. The agreement is striking, reproducing the absence of oscillations in the transient reflectivity and the exact spectral change corresponding to the redshift. The only discrepancy is that the theory predicts a faster rise time of the signal compared to the experiment, which will be discussed

further below. To evidence the role of the dynamic evolution of the Hubbard U parameter, we repeat the calculations while keeping U frozen to its ground-state value – effectively removing these dynamical correlations and keeping other physical effects identical. Importantly, the frozen U calculation still includes all population transfer and local-field effects. Figure 3c displays the resulting transient reflectivity trace, with the signal almost entirely disappearing. Comparing the spectral changes more precisely (Figure 3d) we demonstrate that the experimental redshift is almost entirely due to the renormalization of U . We thus conclude that other effects, typically relevant for weakly-correlated materials, only marginally affect the out-of-equilibrium response of NiO.

Given the precise description of the transient effect by TDDFT+ U calculations, it is interesting to attempt a description of the shift in the Ni $M_{2,3}$ absorption edge using multiplet calculations. Although strictly valid within an adiabatic approach, such simulations offer the advantage of providing an intuitive set of parameters that capture the salient attributes of the transient behavior thus providing a simplified view of the evolution of the local electronic structure. Several assumptions can be adopted to simplify the consideration within the ligand-field approximation (see Methods). We start from parameters that reproduce the experimental static reflectivity (see spectrum in Fig. 1e and SM) and assume that the crystal field remains conserved within the first dozen of fs. Out-of-equilibrium, the Hubbard U used for multiplet calculation is changed from the ground-state value by $\Delta U = -100$ meV, following our TDDFT calculations, and is accompanied by a renormalization of the charge-transfer energy of $\Delta U/2$. First, we find that a rigid shift of the absorption edge is achievable if the hybridization parameters are also modified (see Figure 3e). A 3.3% reduction of the hybridization must be taken into account to reproduce the experimental shift. Furthermore, although the choice of parameters is not unique, for the best description they are linearly constrained to each other. We find that for $\Delta U = -200$ to 0 meV, a change of the hybridization by $(0.0085\Delta U + 4.2)\%$ delivers a satisfactory match of the measured rigid shift (see SM³⁶). Our analysis illustrates how multiplet calculations – which are more accessible than TDDFT+ U – can also be used to reproduce the out-of-equilibrium state of NiO, laying the groundwork for future approaches of correlated materials.

Few-femtosecond screening dynamics

Going back to the experimental results with the U renormalization in mind, we can directly interpret the data to measure the temporal change in the Hubbard parameter, $\Delta U(t)$. As illustrated in Figure 4a,b, $\Delta U(t)$ brings the upper (resp. lower) Hubbard band down (resp. up) in energy by $\Delta U(t)/2$. Therefore, the energy of the $Ni_{3p} \rightarrow$ UHB transition, which is the probe step of the experiment, will be reduced by $\Delta U(t)/2$. The aforementioned redshift thus corresponds to half the change in U . Figure 4c presents the experimentally obtained $\Delta U(t)$, using a least-square fit at each time delay to get the shift value, and compares it with the one calculated from our TDDFT+ U . The agreement in their final magnitude is excellent, confirming again the accuracy of the simulation. The discrepancy, as seen before in Figure 3, lies in an underestimated response time of the system. Experimentally, this response time is comprised of

the instrument response function and of the intrinsic property of the material. The instrument response function was cross-checked using both the transient reflectivity of MgO (see Fig. 2a) and the transient absorption of helium, a common reference system in attosecond spectroscopy.³⁷ The signal was fitted using a functional allowing a non-instantaneous system response³⁸ (see SM), yielding an electronic response time of (7.0 ± 1.5) fs. This timescale is inherent to NiO; however, at this stage it is difficult to precisely point out its nature. At these few-femtosecond timescales, the electronic state of the material is likely not thermalized, making it hard to describe theoretically, especially given the underlying adiabatic approximation used in our TDDFT+U simulations. Some insight can be obtained by comparing with another type of calculations: state-of-the-art extended dynamical mean-field theory (EDMFT) applied to simple yet relevant models.³⁹ Golez et al.⁴⁰ showed that in a single-band $U - V$ Hubbard model subjected to an electric field pulse, the system's response is delayed, occurring on the timescale of electron hopping. This behavior was attributed to the presence of non-local screening, an effect not fully captured by our TDDFT-based approach, which relies on approximate dynamical screening. Although the simple system studied by Golez et al. is less directly comparable to real solids, it suggests an intuitive picture: after a light-induced change in screening, the timescale for the electronic system to reorganize is linked to the Hubbard model's hopping time.

The consequence of this ultrafast interaction quench was then investigated in measurements up to 50 ps. We observe that the photo-induced response that rises in 7 fs induces a long-lived signal. The spectral shape during dynamics at longer times is different from the pure redshift observed in the first few femtoseconds, hinting to a different physical process. Two timescales are measured in the decay process: $\tau_1 = (300 \pm 100)$ fs and $\tau_2 = (6.0 \pm 0.7)$ ps (see raw data and fitting in the Supplemental Material³⁶). After 50 ps, the system has not yet fully returned to equilibrium, and decays at a rate that is too slow for our measurement to resolve. The two measured timescales match very well with the ones from an earlier time-resolved electron diffraction experiment in NiO,⁴¹ disclosing that the two timescales correspond to a transition into a structurally-distorted nonthermal state. The combined information between the two experiments allows to draw a complete picture of the light-driven behavior of NiO: the laser pulse first quenches the onsite electronic interaction within few femtoseconds and reduces the initial antiferromagnetic order. In turn, exchange striction triggers lattice motion towards a more symmetric state, reducing the rhombohedral lattice distortion. The final metastable state is found to be very long-lived, showing that here, strong correlations do not lead to fast thermalization. Such thermalization bottlenecks were already identified in Mott insulators.^{42,43} This scenario would be confirmed by measurements sensitive to the antiferromagnetic order, as well as by modeling the XUV transient reflectivity triggered by the structural change. While it is not directly possible with the theory used here, it is remarkable that the experiment is capable of following accurately the sample dynamics across multiple timescales and connect ultrafast electronic dynamics to long-term spin-lattice coupled processes.

In summary, we have demonstrated that the correlated insulator NiO exhibits a fundamentally different attosecond response to an intense laser field, compared to the band insulator MgO. The fact that we do not observe any field-driven 2ω signal in either experiment or simulations brings forth important questions for

attosecond science, such as the feasibility of lightwave control at optical frequencies⁴⁴ in strongly-correlated systems, in contrast to standard insulators where this was demonstrated in numerous studies.^{45,46} To further strengthen this observation, we also performed CEP-dependent TDDFT simulations (see SM³⁶) and find that the system response does not substantially change with CEP. This demonstrates that the Hubbard U renormalization – the preeminent system response – is driven by the laser intensity and not by its electric field.

More generally, this work provides the first time-resolved observation of light-driven interaction quenching at its natural timescale. We evidence an inherent response time of a few femtoseconds for the process, showing that the U renormalization is extremely fast, but not quite instantaneous. This timescale is a new observable, whose physical origin still needs to be elucidated by more advanced theory and by exploring other strongly-correlated systems. If its nature is confirmed, this timescale would represent the speed at which the electron-electron interaction, or screening, can be manipulated by a laser pulse. The ability to dynamically control the Hubbard U on femtosecond timescales could be foundational for accessing and harnessing new nonequilibrium material states. Finally, this work provides valuable insight for the interpretation of ultrafast phenomena in strongly-correlated materials, such as photo-induced phase transitions^{5,47} or high-harmonic generation.^{11,19,48,49}

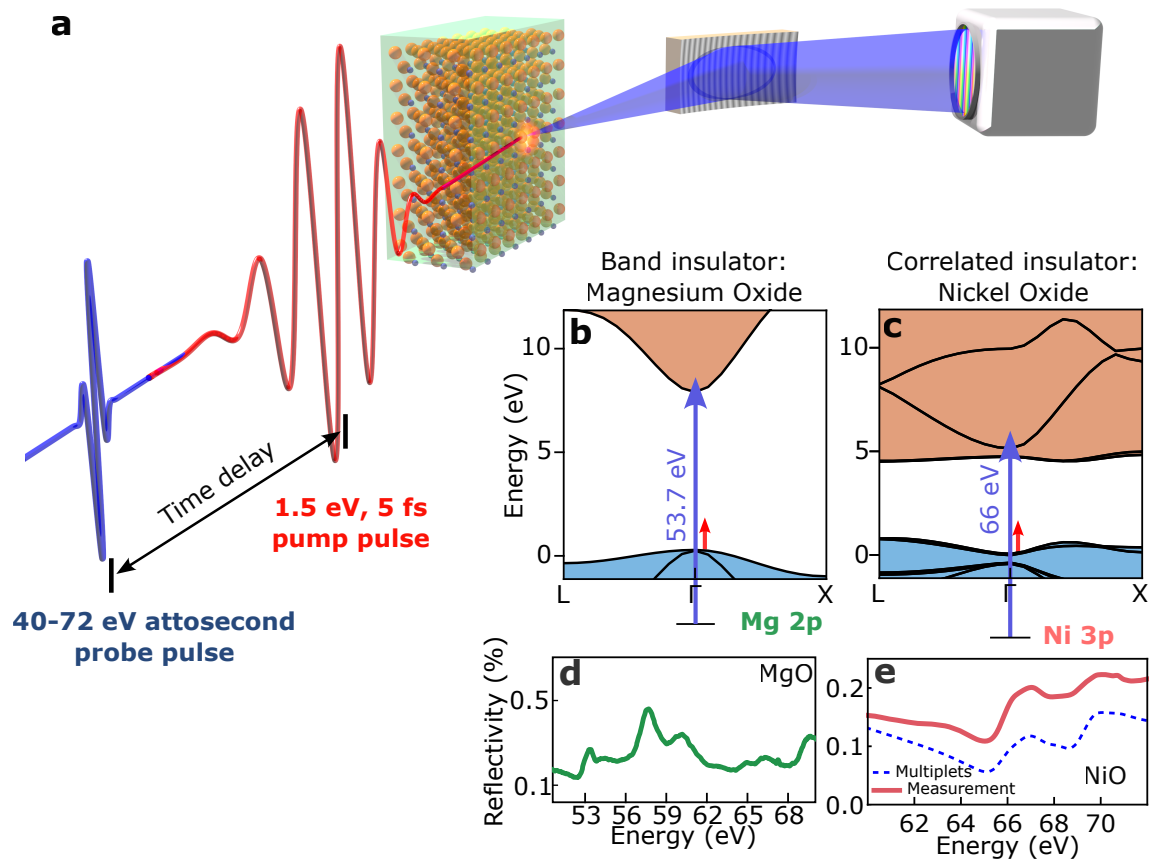


Figure 1 | Principle of the experiment on band and correlated insulators. **a**, Principle of the pump–probe scheme. **b**, **c**, Band structure obtained by LDA for MgO and LDA+U for NiO showing the XUV transition from the Mg 2*p* and Ni 3*p* core levels to their respective conduction bands. The parabolic shape of the MgO conduction band contrasts with the flat band of NiO, the latter being characteristic of strong correlations. **d**, **e**, Measured static reflectivities of both samples, showing the Mg $L_{2,3}$ and the Ni $M_{2,3}$ edges.

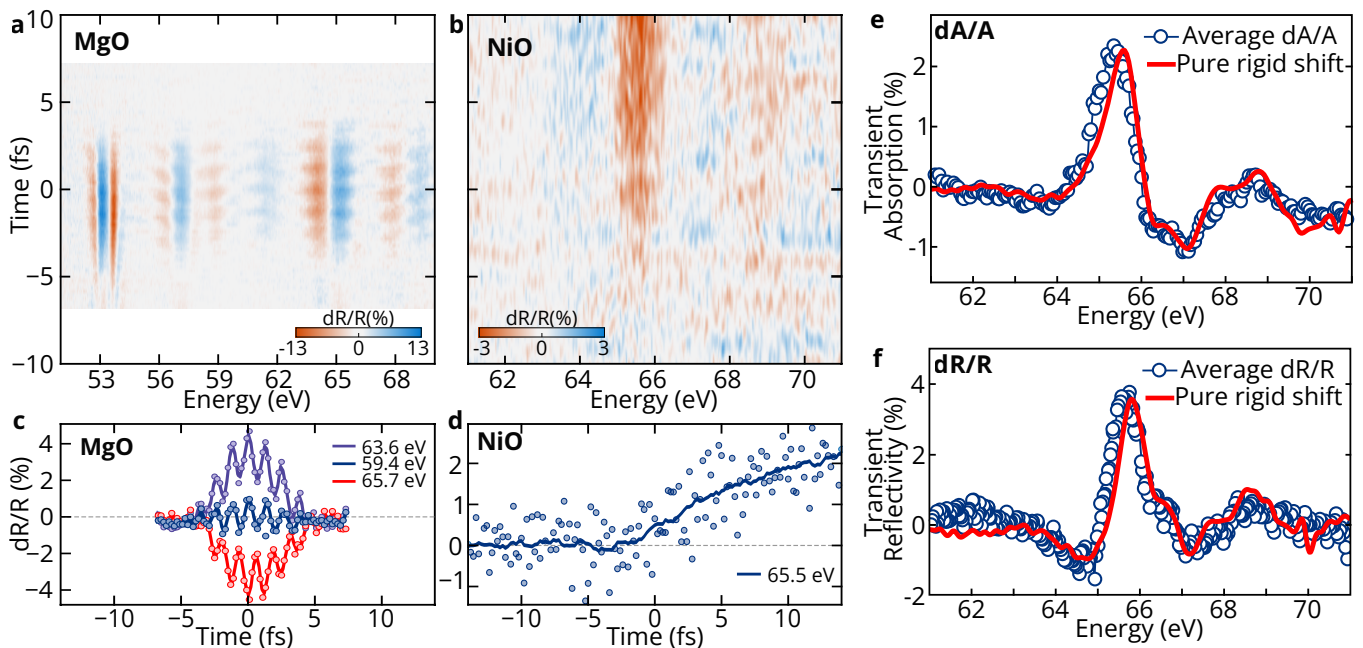


Figure 2 | Attosecond transient reflectivity of MgO and NiO. **a, b,** Experimental transient reflectivity traces for MgO and NiO, as a function of pump-probe delay and XUV energy. Note the very different color scales for the two traces. **c, d,** Temporal slices of the transient reflectivity for MgO and NiO at selected energies. **e,** The experimental transient absorption (open circles, obtained by Kramers-Kronig analysis) is very well reproduced by a pure redshift of the edge absorption (solid red line). Here the red shift is (-51 ± 2) meV. **f,** The experimental transient reflectivity (open circles) is also very well reproduced by a pure redshift (solid red line) of the edge reflectivity. Here the red shift is also (-51 ± 2) meV.

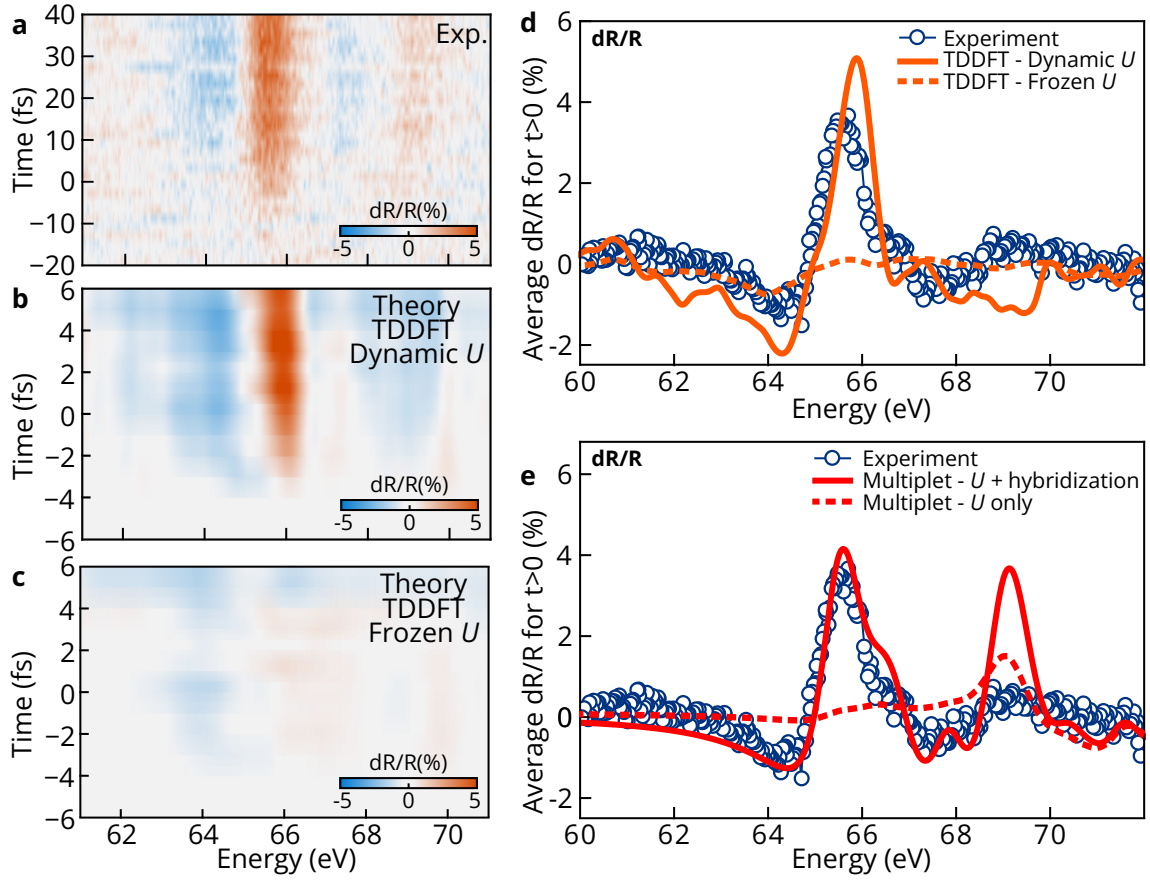


Figure 3 | Importance of dynamical electronic correlations. **a**, Measured transient reflectivity up to 40 fs, showing the full build-up of the signal. **b**, Calculated transient reflectivity by TDDFT+ U calculations when allowing dynamical electronic correlations. Aside from the different timescale (note the vertical axis), the agreement is excellent both in shape and in magnitude. **c**, Same calculation as in **b**, but now considering a frozen U . The color scale is kept the same as in **a** and **b** for comparison. **d**, Averaged transient reflectivity for positive time delays, in the case of the experiment (solid blue line), TDDFT with dynamic U (solid orange line), and TDDFT with frozen U (dashed red line). **e**, Same as **d** but using multiplet calculations, with either a reduction of U only (using the TDDFT value), or with a reduction of hybridization as well (to match the experimental redshift).

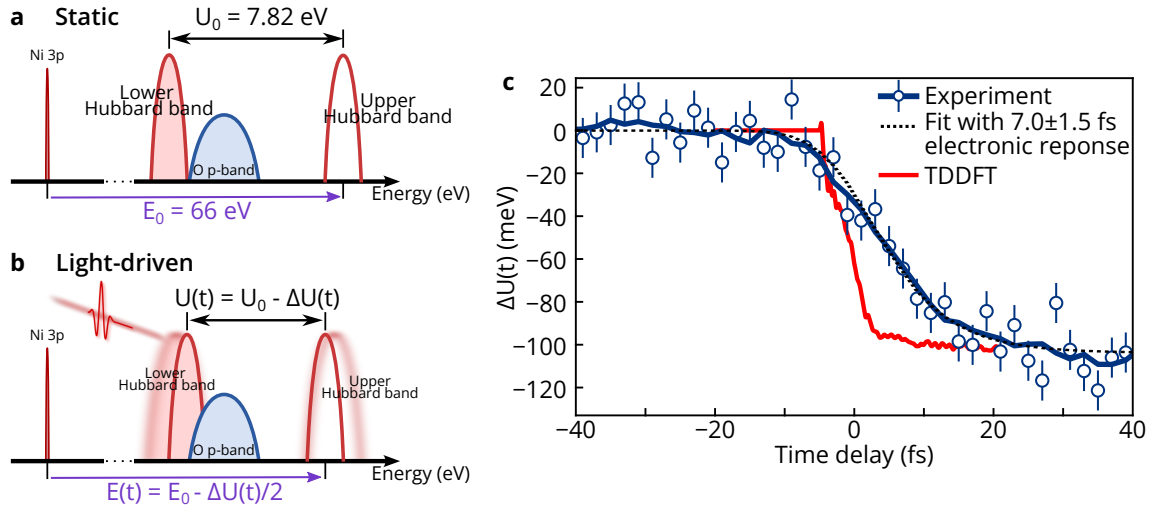


Figure 4 | Timescale of the Hubbard U renormalization. **a**, Schematic band diagram of the system: at equilibrium, the measured signal corresponds to transition from the Ni 3p core-level to the empty upper Hubbard band, which is separated by U_0 from the lower Hubbard band. **b**, Upon photoexcitation, U becomes time-dependent and the energy of the XUV transition is shifted by $\Delta U(t)/2$. **c**, Dynamic evolution of $U(t)$, obtained experimentally (circles and solid blue line) and theoretically (solid red line). The error bars correspond to ± 1 standard deviations. The dashed black line is a fit of the measurement taking into account the experimental time resolution and an inherent system response time - found here to be $(7.0 \pm 1.5) \text{ fs}$.

Methods

TDDFT+U simulations

All the calculations presented here were performed for bulk NiO, which is a type-II antiferromagnetic material below its Néel temperature ($T_N = 523\text{K}$ ⁵⁰). We neglected the small rhombohedral distortions and considered NiO in its cubic rock-salt structure, which does not affect the result of calculated optical spectra. Calculations were performed including spin-orbit coupling using fully norm-conserving pseudopotentials for Ni and O, generated thanks to the Ape code,⁵¹ treating explicitly $3p$, $3d$, and $4s$ orbitals as valence orbitals for Ni, and $2p$ orbitals for O. We employed a lattice parameter of 4.1704 \AA a real-space spacing of $\Delta r = 0.3$ Bohr, and a $16 \times 16 \times 8$ \mathbf{k} -point grid to sample the Brillouin zone. The driving field is taken along the $[100]$ crystallographic direction in all the calculations. We consider a laser pulse of 5.2 fs duration (FWHM), matching the experimental duration, with a sin-square envelope for the vector potential. The experimental carrier wavelength $\lambda = 760$ nm was employed, corresponding to a carrier photon energy of 1.63 eV. In all calculations, we set the carrier envelope phase (CEP) to zero. We checked, see SI, that the CEP has no impact on the light-induced change of the Hubbard U . The time-dependent wavefunctions, electric current, and U_{eff} are computed by propagating generalized Kohn-Sham equations within real-time TDDFT+U, as provided by the Octopus package.⁵² We employed the LDA functional⁵³ for describing the semilocal DFT part, and we computed the effective $U_{\text{eff}} = U - J$ for the O $2p$ (U_{eff}^{2p}) and Ni $3d$ orbitals (U_{eff}^{3d}), using localized atomic orbitals from the corresponding pseudopotentials.³⁵ All calculations are propagated for 13.8 fs after the kick, to avoid spurious numerical effects. A Lorentzian broadening of $\eta = 0.3$ eV is obtained by applying a mask to the time-dependent signal before taking the Fourier transform, to mimic the experimental broadening. The experiment is performed at an intensity of $I_{\text{ext}} \sim 6.0 \text{ TW}\cdot\text{cm}^{-2}$ in vacuum. From this intensity, we obtain the strength of the electric field in vacuum. Due to the experimental geometry and the incidence at the Brewster angle, the strength of the transmitted electric field is obtained from the vacuum one by multiplying it by $1/n$, where $n = 2.33$ is the refractive index of NiO at 760 nm. This determines the strength of the electric displacement \mathbf{D} in matter. The total electric field acting on the electric results from the addition of this external field \mathbf{D} with the induced field \mathbf{E}_{ind} . This induced field is obtained as in Ref.²⁰ by coupling the generalized Kohn-Sham equations to the macroscopic Maxwell equations, allowing to capturing the effect of the macroscopic induced transverse electric field. For each time delay, we propagate the generalized time-dependent Kohn-Sham equations of a time-dependent density functional theory plus Hubbard U (TDDFT+U) framework³⁵ coupled to the macroscopic Maxwell equation and we later “kick” the system at the given time-delay to obtain the optical spectra (see Ref.⁵²). The macroscopic induced vector potential $\mathbf{A}_{\text{ind}}(t)$ is computed from the total electronic current $\mathbf{j}(t)$ (atomic units are used throughout this Letter)

$$\frac{\partial^2}{\partial t^2} \mathbf{A}_{\text{ind}}(t) = \frac{4\pi c}{V} \mathbf{j}(t), \quad (1)$$

where V is the volume of the cell. In order to obtain the vector potential induced by the kick, we subtract from the $\mathbf{A}_{\text{ind}}(t)$ a reference calculation obtained in presence of the driving pump laser field but no kick. The dielectric function is then computed from the knowledge of the kick itself and vector potentials induced by the kick.

The time-dependent generalized Kohn-Sham equation within the adiabatic approximation reads⁵⁴

$$i\frac{\partial}{\partial t}|\psi_{n,\mathbf{k}}(t)\rangle = \left[\frac{(\hat{\mathbf{p}} - \mathbf{A}_{\text{tot}}(t)/c)}{2} + \hat{v}_{\text{ext}} + \hat{v}_{\text{H}}[n(\mathbf{r}, t)] + \hat{v}_{\text{xc}}[n(\mathbf{r}, t)] + \hat{V}_U[n(\mathbf{r}, t), \{n_{mm'}\}] \right] |\psi_{n,\mathbf{k}}(t)\rangle, \quad (2)$$

where $|\psi_{n,\mathbf{k}}\rangle$ is a Pauli-spinor Bloch state with a band index n , at the point \mathbf{k} in the Brillouin zone, \hat{v}_{ext} is the ionic potential, $\mathbf{A}_{\text{tot}}(t)$ is the total vector potential containing the induced one of Eq. 1, \hat{v}_{H} is the Hartree potential, \hat{v}_{xc} is the exchange-correlation potential. \hat{V}_U is the non-local operator for DFT+U that depends on also on the occupation matrix of the localized subspace $\{n_{mm'}\}$, see Ref.³⁵ for more details, including the definition of U , J , and \hat{V}_U .

Multiplet calculations

Our simulations rely on the ligand-field approximation tools released in Refs.^{55,56} For the calculation of the $3p^63d^8 \rightarrow 3p^53d^9$ transitions in the unperturbed case, we adopt the main parameters previously listed for NiO: Hubbard $U = 7.3$ eV, crystal field parameter in octahedral symmetry $10Dq = 0.56$ eV, charge-transfer energy $E_{CT} = 4.7$ eV, hybridization of Ni $3d$ states with O $2p$ states $V_{eg} = 2.06$ eV, $V_{t2g} = 1.21$ eV and 120 meV magnetic exchange interaction. Moreover, while conserving the ab initio calculated values for the $3p$ and $3d$ spin-orbit coupling,^{55,57} the reduction factors applied to the atomic Slater integrals were adapted for the best description of the measured XAS spectrum.²⁷ The latter issued the following reduction factors of F^2 , G^1 and G^3 as 0.70 %, 0.66 % and 0.90 %, respectively. To describe the out-of-equilibrium states, we propose that the variation of the on-site Hubbard repulsion and the charge-transfer energy are linked through the linear relationship $\Delta U = 2\Delta E_{CT}$, in line with our TDDFT +U results. Furthermore, the variation of the hybridization strengths was carried out at a constant V_{eg}/V_{t2g} ratio. This simplification is supported by the hypothesis that the local symmetry is conserved during the first dozen fs.

Experimental setup

The experiment is based on a Ti:Sapphire amplifier delivering 24 fs, 2 mJ pulses at a repetition rate of 1 kHz. The pulses are spectrally broadened using a stretched hollow-core fiber with a diameter of 400 μm and a length of 1.4 m (few-cycle Inc.), filled with a helium gradient ranging from 0 bar to 3.5 bar. The pulse is then compressed using chirped mirrors (PC70, Ultrafast Innovations), yielding a pulse duration of 5 fs FWHM from a homemade dispersion scan setup. The central wavelength is 760 nm which corresponds to an optical cycle duration of 2.5 fs. A detailed scheme of the experiment can be found in the supplementary material.³⁶ 80% of the beam is focused in an argon gas cell to generate a continuous XUV spectrum

spanning from 40 eV to 72.5 eV serving as the probe beam. An aluminum dot filter filters out the driving infrared laser and lets a ring of infrared light that is latter used for active stabilization of the delay. The probe is then focused using a toroidal mirror in a 2f-2f configuration. The remaining 20% serves as the pump beam. It is recombined co-linearly with the XUV beam using a doubly drilled mirror. The pump and probe are then focused on the sample, with a measured pump intensity of 6 TW cm^{-2} . The infrared light is then filtered out, and the XUV spectrum is recorded by a spectrometer made of a grating and a XUV CCD camera (greateyes GmbH). Delay stabilization is achieved by locking onto spatial fringes made from the unused pump and probe infrared beams. We use an interferometric filter centered at 790 nm with a width of 10 nm to increase the duration of the pulse significantly, which extend the range of measurement of the delay. The final delay stability is 100 as over several hours. The CEP of the laser is not stabilized. However, this does not prevent the measurement of sub-cycle features as demonstrated by our MgO measurements and previous experiments. All data were acquired thanks to the open source python-based software PyMoDAQ.⁵⁸

Data Availability

The data presented in the manuscript are available from the authors upon request.

Acknowledgements

We would like to thank Iris Crassee for helpful discussions on RefFIT and Siarhei Dziarzhyski for valuable discussions and for providing the sample. This work was supported by the European Union (ERC, Spinfield, Project No. 101041074 and Horizon 2020 Programme No. EU-H2020-LASERLAB-EUROPE-654148), the French Agence Nationale pour la Recherche (under grants TOCYDYS, ANR-19-CE30-0015-01 and HELIMAG, ANR-21-CE30-0037) and the Investissements d’Avenir program of LabEx PALM (ANR-10-LABX-0039-PALM). AA acknowledges the financial support from the Doctoral School ED 388 Chimie-Physique et Chimie Analytique de Paris Centre.

Author contributions

R.C., A.A., M.G., S.G., S.G.C. and R.G. performed the experiments. S.G.C. and R.G. initiated the study. R.C., A.A., C.J.K. and R.G. analyzed the experimental data. F.L. and O.T. operated the laser system. A.R. and N.T.D. performed the TDDFT calculations and first proposed the physical interpretation. A.A. and S.G.C. performed the multiplet calculations. R.C., N.T.D. and R.G. wrote the first version of the manuscript, to which all authors contributed.

[1] E. Dagotto and Y. Tokura, Strongly correlated electronic materials: Present and future, *MRS Bulletin* **33**, 1037–1045 (2008).

- [2] S. Paschen and Q. Si, Quantum phases driven by strong correlations, [Nature Reviews Physics](#) **3**, 9 (2021).
- [3] A. Cavalleri, C. Tóth, C. W. Siders, J. A. Squier, F. Ráksi, P. Forget, and J. C. Kieffer, Femtosecond structural dynamics in VO₂ during an ultrafast solid-solid phase transition, [Phys. Rev. Lett.](#) **87**, 237401 (2001).
- [4] A. de la Torre, D. M. Kennes, M. Claassen, S. Gerber, J. W. McIver, and M. A. Sentef, Colloquium: Nonthermal pathways to ultrafast control in quantum materials, [Rev. Mod. Phys.](#) **93**, 041002 (2021).
- [5] A. S. Johnson, D. Perez-Salinas, K. M. Siddiqui, S. Kim, S. Choi, K. Volckaert, P. E. Majchrzak, S. Ulstrup, N. Agarwal, K. Hallman, R. F. Haglund, C. M. Günther, B. Pfau, S. Eisebitt, D. Backes, F. Maccherozzi, A. Fitzpatrick, S. S. Dhesi, P. Gargiani, M. Valvidares, N. Artrith, F. de Groot, H. Choi, D. Jang, A. Katoch, S. Kwon, S. H. Park, H. Kim, and S. E. Wall, Ultrafast x-ray imaging of the light-induced phase transition in VO₂, [Nature Physics](#) **19**, 215 (2023).
- [6] A. Cavalleri, Photo-induced superconductivity, [Contemporary Physics](#) **59**, 31 (2018).
- [7] S. Fava, G. De Vecchi, G. Jotzu, M. Buzzi, T. Gebert, Y. Liu, B. Keimer, and A. Cavalleri, Magnetic field expulsion in optically driven YBa₂Cu₃O_{6.48}, [Nature](#) **632**, 75 (2024).
- [8] L. Stojchevska, I. Vaskivskiy, T. Mertelj, P. Kusar, D. Svetin, S. Brazovskii, and D. Mihailovic, Ultrafast switching to a stable hidden quantum state in an electronic crystal, [Science](#) **344**, 177 (2014).
- [9] J. Maklar, J. Sarkar, S. Dong, Y. A. Gerasimenko, T. Pincelli, S. Beaulieu, P. S. Kirchmann, J. A. Sobota, S. Yang, D. Leuenberger, R. G. Moore, Z.-X. Shen, M. Wolf, D. Mihailovic, R. Ernstorfer, and L. Rettig, Coherent light control of a metastable hidden state, [Science Advances](#) **9**, eadi4661 (2023).
- [10] J. Bloch, A. Cavalleri, V. Galitski, M. Hafezi, and A. Rubio, Strongly correlated electron–photon systems, [Nature](#) **606**, 41 (2022).
- [11] R. E. F. Silva, I. V. Blinov, A. N. Rubtsov, O. Smirnova, and M. Ivanov, High-harmonic spectroscopy of ultrafast many-body dynamics in strongly correlated systems, [Nature Photonics](#) **12**, 266 (2018).
- [12] M. Schultze, K. Ramasesha, C. D. Pemmaraju, S. A. Sato, D. Whitmore, A. Gandman, J. S. Prell, L. J. Borja, D. Prendergast, K. Yabana, D. M. Neumark, and S. R. Leone, Attosecond band-gap dynamics in silicon, [Science](#) **346**, 1348 (2014).
- [13] G. Inzani, L. Adamska, A. Eskandari-asl, N. Di Palo, G. L. Dolso, B. Moio, L. J. D’Onofrio, A. Lamperti, A. Molle, R. Borrego-Varillas, M. Nisoli, S. Pittalis, C. A. Rozzi, A. Avella, and M. Lucchini, Field-driven attosecond charge dynamics in germanium, [Nature Photonics](#) **17**, 1059 (2023).
- [14] M. Schultze, E. M. Bothschafter, A. Sommer, S. Holzner, W. Schweinberger, M. Fiess, M. Hofstetter, R. Kienberger, V. Apalkov, V. S. Yakovlev, M. I. Stockman, and F. Krausz, Controlling dielectrics with the electric field of light., [Nature](#) **493**, 75 (2013).
- [15] M. Lucchini, S. A. Sato, A. Ludwig, J. Herrmann, M. Volkov, L. Kasmi, Y. Shinohara, K. Yabana, L. Gallmann, and U. Keller, Attosecond dynamical Franz-Keldysh effect in polycrystalline diamond, [Science](#) **353**, 916 (2016).
- [16] A. P. Jauho and K. Johnsen, Dynamical Franz-Keldysh effect, [Physical Review Letters](#) **10.1103/PhysRevLett.76.4576** (1996).
- [17] M. Volkov, S. A. Sato, A. Niedermayr, A. Rubio, L. Gallmann, and U. Keller, Floquet-Bloch resonances in near-petahertz electroabsorption spectroscopy of SiO₂, [Phys. Rev. B](#) **107**, 184304 (2023).
- [18] N. F. Mott, The Basis of the Electron Theory of Metals, with Special Reference to the Transition Metals, [Proceedings of the Physical Society. Section A](#) **62**, 416 (1949).
- [19] N. Tancogne-Dejean, M. A. Sentef, and A. Rubio, Ultrafast modification of Hubbard U in a strongly correlated material: Ab initio high-harmonic generation in NiO, [Phys. Rev. Lett.](#) **121**, 097402 (2018).

- [20] N. Tancogne-Dejean, M. A. Sentef, and A. Rubio, Ultrafast transient absorption spectroscopy of the charge-transfer insulator NiO: Beyond the dynamical Franz-Keldysh effect, *Physical Review B* **102**, 115106 (2020).
- [21] C. J. Kaplan, P. M. Kraus, A. D. Ross, M. Zürich, S. K. Cushing, M. F. Jager, H.-T. Chang, E. M. Gullikson, D. M. Neumark, and S. R. Leone, Femtosecond tracking of carrier relaxation in germanium with extreme ultraviolet transient reflectivity, *Physical Review B* **97**, 205202 (2018).
- [22] D. M. Roessler and W. C. Walker, Electronic spectrum and ultraviolet optical properties of crystalline mgo, *Phys. Rev.* **159**, 733 (1967).
- [23] S. Hüfner, Electronic structure of NiO and related 3d-transition-metal compounds, *Advances in Physics* **43**, 183 (1994).
- [24] R. Gêneaux, C. J. Kaplan, L. Yue, A. D. Ross, J. E. Bækhoj, P. M. Kraus, H.-T. Chang, A. Guggenmos, M.-Y. Huang, M. Zürich, K. J. Schafer, D. M. Neumark, M. B. Gaarde, and S. R. Leone, Attosecond Time-Domain Measurement of Core-Level-Exciton Decay in Magnesium Oxide, *Physical Review Letters* **124**, 207401 (2020).
- [25] M. Lucchini, S. A. Sato, G. D. Lucarelli, B. Moio, G. Inzani, R. Borrego-Varillas, F. Frassetto, L. Poletto, H. Hübener, U. De Giovannini, A. Rubio, and M. Nisoli, Unravelling the intertwined atomic and bulk nature of localised excitons by attosecond spectroscopy, *Nature Communications* **12**, 1021 (2021).
- [26] A. B. Kuzmenko, Kramers–Kronig constrained variational analysis of optical spectra, *Review of Scientific Instruments* **76**, 083108 (2005).
- [27] S. G. Chiuzbăian, G. Ghiringhelli, C. Dallera, M. Grioni, P. Amann, X. Wang, L. Braicovich, and L. Patthey, Localized electronic excitations in nio studied with resonant inelastic x-ray scattering at the Ni *M* threshold: Evidence of spin flip, *Physical Review Letters* **95**, 197402 (2005).
- [28] M. Zürich, H.-T. Chang, L. J. Borja, P. M. Kraus, S. K. Cushing, A. Gandman, C. J. Kaplan, M. H. Oh, J. S. Prell, D. Prendergast, C. D. Pemmaraju, D. M. Neumark, and S. R. Leone, Direct and simultaneous observation of ultrafast electron and hole dynamics in germanium, *Nature Communications* **8**, 15734 (2017).
- [29] H.-T. Chang, A. Guggenmos, S. K. Cushing, Y. Cui, N. U. Din, S. R. Acharya, I. J. Porter, U. Kleineberg, V. Turkowski, T. S. Rahman, D. M. Neumark, and S. R. Leone, Electron thermalization and relaxation in laser-heated nickel by few-femtosecond core-level transient absorption spectroscopy, *Physical Review B* **103**, 064305 (2021).
- [30] X. Wang, R. Y. Engel, I. Vaskivskiy, D. Turenne, V. Shokeen, A. Yaroslavtsev, O. Grånäs, R. Knut, J. O. Schunck, S. Dziarzhytski, G. Brenner, R.-P. Wang, M. Kuhlmann, F. Kuschewski, W. Bronsch, C. Schüßler-Langeheine, A. Styervoyedov, S. S. P. Parkin, F. Parmigiani, O. Eriksson, M. Beye, and H. A. Dürr, Ultrafast manipulation of the NiO antiferromagnetic order via sub-gap optical excitation, *Faraday Discuss.* **237**, 300 (2022).
- [31] O. Grånäs, I. Vaskivskiy, X. Wang, P. Thunström, S. Ghimire, R. Knut, J. Söderström, L. Kjellsson, D. Turenne, R. Y. Engel, M. Beye, J. Lu, D. J. Higley, A. H. Reid, W. Schlotter, G. Coslovich, M. Hoffmann, G. Kolesov, C. Schüßler-Langeheine, A. Styervoyedov, N. Tancogne-Dejean, M. A. Sentef, D. A. Reis, A. Rubio, S. S. P. Parkin, O. Karis, J.-E. Rubensson, O. Eriksson, and H. A. Dürr, Ultrafast modification of the electronic structure of a correlated insulator, *Phys. Rev. Res.* **4**, L032030 (2022).
- [32] T. Lojewski, D. Golez, K. Ollefs, L. L. Guyader, L. Kämmerer, N. Rothenbach, R. Y. Engel, P. S. Miedema, M. Beye, G. S. Chiuzbăian, R. Carley, R. Gort, B. E. V. Kuiken, G. Mercurio, J. Schlappa, A. Yaroslavtsev, A. Scherz, F. Döring, C. David, H. Wende, U. Bovensiepen, M. Eckstein, P. Werner, and A. Eschenlohr, Photo-induced charge-transfer renormalization in NiO, *arXiv* , 2305.10145 (2024).

- [33] S. Beaulieu, S. Dong, N. Tancogne-Dejean, M. Dendzik, T. Pincelli, J. Maklar, R. P. Xian, M. A. Sentef, M. Wolf, A. Rubio, L. Rettig, and R. Ernstorfer, Ultrafast dynamical lifshitz transition, *Science Advances* **7**, eabd9275 (2021).
- [34] D. R. Baykusheva, H. Jang, A. A. Husain, S. Lee, S. F. R. TenHuisen, P. Zhou, S. Park, H. Kim, J.-K. Kim, H.-D. Kim, M. Kim, S.-Y. Park, P. Abbamonte, B. J. Kim, G. D. Gu, Y. Wang, and M. Mitrano, Ultrafast renormalization of the on-site coulomb repulsion in a cuprate superconductor, *Phys. Rev. X* **12**, 011013 (2022).
- [35] N. Tancogne-Dejean, M. J. T. Oliveira, and A. Rubio, Self-consistent DFT + U method for real-space time-dependent density functional theory calculations, *Phys. Rev. B* **96**, 245133 (2017).
- [36] See Supplemental Material at, See Supplemental Material at.
- [37] C. Ott, A. Kaldun, L. Argenti, P. Raith, K. Meyer, M. Laux, Y. Zhang, A. Blättermann, S. Hagstotz, T. Ding, R. Heck, J. Madroñero, F. Martín, and T. Pfeifer, Reconstruction and control of a time-dependent two-electron wave packet, *Nature* **516**, 374 (2014).
- [38] B. R. de Roulet, L. Drescher, S. A. Sato, and S. R. Leone, Initial electron thermalization in metals measured by attosecond transient absorption spectroscopy, *Phys. Rev. B* **110**, 174301 (2024).
- [39] Y. Murakami, D. Golež, M. Eckstein, and P. Werner, Photo-induced nonequilibrium states in mott insulators, *arXiv* , 2310.05201 (2023).
- [40] D. Golež, M. Eckstein, and P. Werner, Dynamics of screening in photodoped mott insulators, *Phys. Rev. B* **92**, 195123 (2015).
- [41] Y. W. Windsor, D. Zahn, R. Kamrta, J. Feldl, H. Seiler, C.-T. Chiang, M. Ramsteiner, W. Widdra, R. Ernstorfer, and L. Rettig, Exchange-striction driven ultrafast nonthermal lattice dynamics in NiO, *Phys. Rev. Lett.* **126**, 147202 (2021).
- [42] C. Kollath, A. M. Läuchli, and E. Altman, Quench dynamics and nonequilibrium phase diagram of the Bose-Hubbard model, *Phys. Rev. Lett.* **98**, 180601 (2007).
- [43] M. Eckstein, M. Kollar, and P. Werner, Thermalization after an interaction quench in the Hubbard model, *Phys. Rev. Lett.* **103**, 056403 (2009).
- [44] M. Borsch, M. Meierhofer, R. Huber, and M. Kira, Lightwave electronics in condensed matter, *Nature Reviews Materials* **8**, 668 (2023).
- [45] V. Hanus, V. Csajbók, Z. Pápa, J. Budai, Z. Márton, G. Z. Kiss, P. Sándor, P. Paul, A. Szeghalmi, Z. Wang, B. Bergues, M. F. Kling, G. Molnár, J. Volk, and P. Dombi, Light-field-driven current control in solids with pJ-level laser pulses at 80 MHz repetition rate, *Optica* **8**, 570 (2021).
- [46] M. Ossiander, K. Golyari, K. Scharl, L. Lehnert, F. Siegrist, J. P. Bürger, D. Zimin, J. A. Gessner, M. Weidman, I. Floss, V. Smejkal, S. Donsa, C. Lemell, F. Libisch, N. Karpowicz, J. Burgdörfer, F. Krausz, and M. Schultze, The speed limit of optoelectronics, *Nature Communications* **13**, 1620 (2022).
- [47] M. F. Jager, C. Ott, P. M. Kraus, C. J. Kaplan, W. Pouse, R. E. Marvel, R. F. Haglund, D. M. Neumark, and S. R. Leone, Tracking the insulator-to-metal phase transition in VO₂ with few-femtosecond extreme UV transient absorption spectroscopy, *Proceedings of the National Academy of Sciences* **114**, 9558 (2017).
- [48] C. Shao, H. Lu, X. Zhang, C. Yu, T. Tohyama, and R. Lu, High-harmonic generation approaching the quantum critical point of strongly correlated systems, *Phys. Rev. Lett.* **128**, 047401 (2022).
- [49] K. Uchida, G. Mattoni, S. Yonezawa, F. Nakamura, Y. Maeno, and K. Tanaka, High-order harmonic generation and its unconventional scaling law in the mott-insulating Ca₂RuO₄, *Phys. Rev. Lett.* **128**, 127401 (2022).
- [50] A. P. Cracknell and S. J. Joshua, The space group corepresentations of antiferromagnetic NiO, *Mathematical Proceedings of the Cambridge Philosophical Society* **66**, 493 (1969).

- [51] M. J. Oliveira and F. Nogueira, Generating relativistic pseudo-potentials with explicit incorporation of semi-core states using ape, the atomic pseudo-potentials engine, *Computer Physics Communications* **178**, 524 (2008).
- [52] N. Tancogne-Dejean, M. J. T. Oliveira, X. Andrade, H. Appel, C. H. Borca, G. Le Breton, F. Buchholz, A. Castro, S. Corni, A. A. Correa, U. De Giovannini, A. Delgado, F. G. Eich, J. Flick, G. Gil, A. Gomez, N. Helbig, H. Hübener, R. Jestädt, J. Jornet-Somoza, A. H. Larsen, I. V. Lebedeva, M. Lüders, M. A. L. Marques, S. T. Ohlmann, S. Pipolo, M. Rampp, C. A. Rozzi, D. A. Strubbe, S. A. Sato, C. Schäfer, I. Theophilou, A. Welden, and A. Rubio, Octopus, a computational framework for exploring light-driven phenomena and quantum dynamics in extended and finite systems, *The Journal of Chemical Physics* **152**, 124119 (2020).
- [53] J. P. Perdew and A. Zunger, Self-interaction correction to density-functional approximations for many-electron systems, *Phys. Rev. B* **23**, 5048 (1981).
- [54] The nonlocal part of the pseudopotential is omitted for conciseness.
- [55] M. W. Haverkort, M. Zwierzycki, and O. K. Andersen, Multiplet ligand-field theory using wannier orbitals, *Phys. Rev. B* **85**, 165113 (2012).
- [56] M. W. Haverkort, Documentation - quanta, <https://www.quanta.org/documentation/start> (2017), last modified: 2017/03/01.
- [57] G. Van der Laan, M2, 3 absorption spectroscopy of 3d transition-metal compounds, *Journal of Physics: Condensed Matter* **3**, 7443 (1991).
- [58] S. Weber, Pymodaq: An open-source python-based software for modular data acquisition, *Review of Scientific Instruments* **92** (2021).